

Enhanced electro-optical lithium niobate photonic crystal wire waveguide on a smart-cut thin film

H. Lu,¹ B. Sadani,¹ N. Courjal,¹ G. Ulliac,¹ N. Smith,² V. Stenger,² M. Collet,¹ F. I. Baida,¹ and M.-P. Bernal^{1,*}

¹Institut FEMTO-ST, UMR 6174, Département d'Optique, 16 Route de Gray, 25030 Besançon Cedex, France

²SRICO, 2724 Sawbury Blvd. Columbus, Ohio 43235-4579, USA

*maria-pilar.bernal@univ-fcomte.fr

Abstract: We report an electro-optically tunable photonic crystal linear cavity etched on a 200 nm lithium niobate waveguide ridge. The photonic crystal cavity and the ridge are both fabricated on a 1 μm thin film of lithium niobate obtained by smart-cut technology. The photonic crystal, of area $4 \times 0.8 \mu\text{m}^2$, has been engineered to work in a slow light configuration so that the electro-optic effect is 20 times more important than in bulk material.

©2012 Optical Society of America

OCIS codes: (130.0250) Optoelectronics; (310.0310) Thin films; (130.3730) Lithium niobate; (160.5298) Photonic crystals.

References and links

1. M. Soljacić and J. D. Joannopoulos, "Enhancement of nonlinear effects using photonic crystals," *Nat. Mater.* **3**(4), 211–219 (2004).
2. F. Lacour, N. Coujal, M.-P. Bernal, A. Sabac, C. Bainier, and M. Spajer, "Nanostructuring lithium niobate substrates by focused ion beam milling," *Opt. Mater.* **27**(8), 1421–1425 (2005).
3. M. Roussey, M.-P. Bernal, N. Courjal, D. Van Labeke, F. I. Baida, and R. Salut, "Electro-optic effect exaltation on lithium niobate photonic crystals due to slow photons," *Appl. Phys. Lett.* **89**(24), 241110 (2006).
4. M. Roussey, F. I. Baida, and M.-P. Bernal, "Experimental and theoretical observations of the slow-light effects on a tunable photonic crystal," *J. Opt. Soc. Am. B* **24**(6), 1416–1422 (2007).
5. J. Amet, G. Ulliac, F. I. Baida, and M.-P. Bernal, "Experimental evidence of enhanced electro-optic control on a lithium niobate photonic crystal superprism," *Appl. Phys. Lett.* **96**(10), 103111 (2010).
6. M. Levy, R. M. Osgood, R. Liu, L. E. Cross, G. S. Cargill III, A. Kumar, and H. Bakhru, "Fabrication of single-crystal lithium niobate films by crystal ion slicing," *Appl. Phys. Lett.* **73**(16), 2293–2295 (1998).
7. A. M. Radojevic, M. Levy, H. Kwak, and R. M. Osgood, Jr., "Strong nonlinear optical response in epitaxial liftoff single-crystal LiNbO₃ films," *Appl. Phys. Lett.* **75**(19), 2888–2890 (1999).
8. D. W. Ward, E. R. Statz, K. A. Nelson, R. M. Roth, and R. M. Osgood, "Terahertz wave generation and propagation in thin-film lithium niobate produced by crystal ion slicing," *Appl. Phys. Lett.* **86**(2), 022908 (2005).
9. D. Djukic, G. Cerda-Pons, R. M. Roth, R. M. Osgood, Jr., S. Bakhru, and H. Bakhru, "Electro-optically tunable second-harmonic-generation gratings in ion-exfoliated thin films of periodically poled lithium niobate," *Appl. Phys. Lett.* **90**(17), 171116 (2007).
10. A. M. Radojevic, M. Levy, R. M. Osgood, Jr., D. H. Jundt, A. Kumar, and H. Bakhru, "Second-order optical nonlinearity of 10- μm -thick periodically poled LiNbO₃ films," *Opt. Lett.* **25**(14), 1034–1036 (2000).
11. T. Izuhara, R. Roth, R. M. Osgood, Jr., S. Bakhru, and H. Bakhru, "Low-voltage tunable TE/TM converter on ion-sliced lithium niobate thin film," *Electron. Lett.* **39**(15), 1118–1119 (2003).
12. P. Rabiei and P. Günter, "Optical and electro-optical properties of submicrometer lithium niobate slab waveguides prepared by crystal ion slicing and wafer bonding," *Appl. Phys. Lett.* **85**(20), 4603–4605 (2004).
13. G. Poberaj, M. Koechlin, F. Sulser, A. Guarino, J. Hajfler, and P. Günter, "Ion-sliced lithium niobate thin films for active photonic devices," *Opt. Mater.* **31**(7), 1054–1058 (2009).
14. F. Sulser, G. Poberaj, M. Koechlin, and P. Günter, "Photonic crystal structures in ion-sliced lithium niobate thin films," *Opt. Express* **17**(22), 20291–20300 (2009).
15. R. Geiss, S. Diziain, R. Iliew, C. Etrich, H. Hartung, N. Janunts, F. Schrepel, F. Lederer, T. Pertsch, and E.-B. Kley, "Light propagation in a free-standing lithium niobate photonic crystal waveguide," *Appl. Phys. Lett.* **97**(13), 131109 (2010).
16. W. Liu, D. Zhan, X. Ma, Z. Song, and S. Feng, "Fabrication of single-crystalline LiTaO₃ film on silicon substrate using thin film transfer technology," *J. Vac. Sci. Technol. B* **26**(1), 206 (2008).
17. P. Murali, "Micro machined infrared detectors based on pyroelectric thin films," *Rep. Prog. Phys.* **64**(10), 1339–1388 (2001).

18. N. Chandrasekaran, T. Soga, and T. Jimbo, "GaAs film on Si substrate transplanted from GaAs/Ge structure by direct bonding," *Appl. Phys. Lett.* **82**(22), 3892–3894 (2003).
 19. P. Rabiei and W. H. Steier, "Lithium niobate ridge waveguides and modulators fabricated using smart guide," *Appl. Phys. Lett.* **86**(16), 161115 (2005).
 20. T. A. Ramadan, M. Levy, and R. M. Osgood, Jr., "Electro-optic modulation in crystal-ion-sliced z-cut LiNbO₃ thin films," *Appl. Phys. Lett.* **76**(11), 1407–1409 (2000).
-

Introduction

Enormous progress in photonic crystal fabrication has been shown in silicon and other semiconductor materials. The success of the realizations is due to the recent development in micro and nanostructuring of the semiconductor technology. However, in order to have an integrated photonic chip containing all optical functionalities, nano photonic devices based on non-linear materials offering the possibility of modulation and switching are essential [1].

Lithium Niobate (LiNbO₃), LN, is a nonlinear ferroelectric material extensively used in optoelectronics and surface acoustic wave devices. The fabrication of LN photonic crystals can potentially decrease the size of crucial components in many optical systems. Achieving LN photonic crystal structures requires high index contrast materials to create vertical and in-plane index confinement, which is difficult with waveguiding fabrication techniques such as diffusion or proton exchange methods.

Annealed Proton Exchange (APE) LN waveguides have small refractive index contrast resulting in a weak light confinement and a broadly distributed mode with its center located 1.5 μm below the crystal surface. Thus, air holes with high aspect ratio are required. FIB milling of cylindrical holes with high aspect ratio in LN is a difficult task due to redeposition effects of the Lithium compound [2].

LN photonic crystal slab structures would be an elegant way of realizing high-density integrated optical systems and low-loss large bandwidth nonlinear devices. The optical properties can then be externally tuned by applying for instance an electric field (via the Pockels effect). In addition, Pockels effect in LN is much faster than carrier induced index changes in silicon-on-insulator (SOI) structures. LN electro-optic photonic crystal structures allow applications requiring high switching speeds that would be difficult to obtain in other materials. Moreover, thanks to specific slow light geometries, we have already demonstrated that the needed external field can be greatly reduced [3–5].

This required stronger vertical confinement of guided light offered by slab structures can be achieved using LN micrometric thickness films on low-index substrate materials. But, if one wants to use them for dynamical optical functions such as electro-optical devices, these layers must keep identical physical properties as one could find in LN commercial wafers (which are single-crystal).

The best technology up to date to achieve this is the so called crystal ion slicing or smart cut, which is based on selective ion implantation. Two groups have extensively developed it; Osgood's and Günther's groups. The difference between them is the etching method to release the LN thin layer from its bulk substrate.

Osgood's group is the pioneer in thin films by smart cut [6]. Their thickness is restricted to 10 μm . They have verified that the linear and nonlinear properties are identical to bulk material [7]. They have used the films for THz polariton generation [8], electro-optically tunable second-harmonic generation grating in thin films [9] of periodically poled LN [10], and low voltage tunable TE/TM converter [11].

Günther's group has also developed LN thin films bonded in SiO₂ and adhesive polymer benzocyclobutene (BCB) obtaining thickness under 1 μm [12] which has allowed them to fabricate electro-optic tunable micro-ring resonators [13] and passive photonic crystals [14].

Some other recent demonstrations of photonic crystals in lithium niobate have been done in thin films or in suspended LN slabs but in any of these works optical far field transmission has been reported [15].

In this work, we report on a submicrometric-size electro-optically tunable photonic crystal linear cavity in which tunability is greatly enhanced due to the appropriate choice of a slow light geometry. The active element has only a size of $4 \times 0.8 \mu\text{m}^2$. The horizontal light

confinement is achieved thanks to a wire waveguide fabricated by RIE (Reactive Ion Etching) on the LN thin layer of 800 nm width and 200 nm thickness. This waveguide has been etched on a smart-cut 1 μm thickness single-crystal lithium niobate. The photonic crystal fabricated is just one line on holes following the light propagation direction with a defect in the middle.

2. Numerical analysis

2.1 Numerical analysis of the wire waveguide

Thin films of lithium niobate with an intermediate BCB layer act as planar waveguides. In order to avoid diffraction effects, horizontal light confinement has to be provided. In the first place we have performed numerical simulations with the commercial software BeamProp (RSoft) in order to obtain the appropriate waveguide geometry to host the photonic crystal. Schematic of the modeled structure is shown in Fig. 1(a). The 1 micron lithium niobate layer of thickness “H” as well as a polymer barrier layer (BCB) has been taken into account. Waveguide width of 800 nm has been assumed (this value is determined by our technological constraints) and the varying parameter has been the ridge height “h”. The transverse mode profile is shown in Fig. 1(b) to (e) respectively, where h varies from 100 nm to 400 nm. We can clearly see that as the ridge height increases the mode is more confined in the horizontal direction.

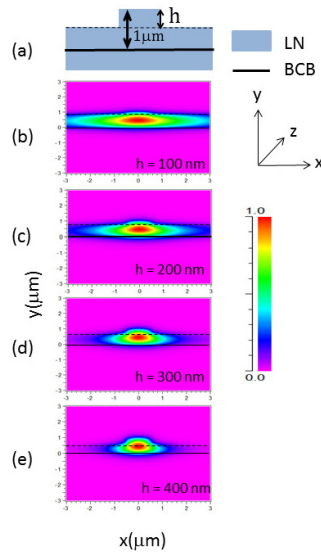


Fig. 1. (a) Schematic of the simulated waveguide. Index profile of the guided mode for ridge waveguides of thicknesses 100 (b), 200 (c), 300 (d), and 400 nm (e) respectively. The BCB layer starts at vertical position 0 μm (continuous line) and the bottom surface of the ridge waveguide is delimited by the discontinuous line.

We choose 200 nm ridge height since the horizontal dimension of the effective mode will provide a good interaction with the photonic crystal that will be etched on it (85% of the optical intensity extends into the photonic crystal). A stronger confinement could lead a higher interaction and therefore a higher effective electro-optical effect. However, 200 nm height represents a good compromise between technological constraints and fear confinement.

2.2 Numerical analysis of the photonic crystal

The slow light geometry is based on Fabry-Perot photonic crystal geometry as shown in Fig. 2(a). One line of defect is created perpendicular to the light propagation direction. Planar Waveguide Expansion (PWE) numerical simulation method has been used to calculate the dispersion relation using the design of Fig. 2(a) as the supercell. Results are shown in Fig. 2(b) where normalized frequency is shown for the ΓM direction. It can clearly be observed

that there is a flat cavity mode inside the photonic band gap (PBG) for a normalized frequency $a/\lambda = 0.32$ (a being the hole periodicity and λ the input wavelength). For a transmitted mode at $\lambda = 1550$ nm holes with a periodicity $a = 508$ nm ($r/a = 0.35$, $r =$ hole radius) have to be fabricated. Flat modes imply low group velocities and, if chosen in an active material such as lithium niobate, Pockels effect can be greatly enhanced. This enhancement is quantified with the local field factor [3,4].

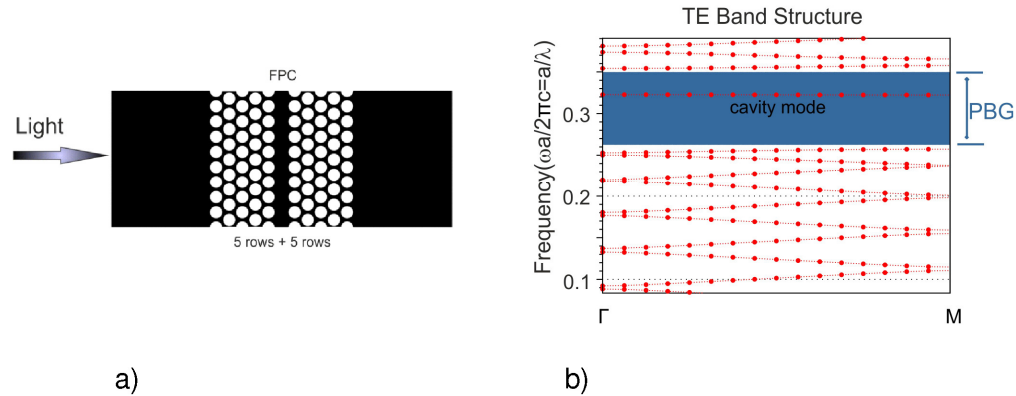


Fig. 2. (a) Modeled supercell by the PWE method, and (b) dispersion relation of the photonic crystal.

Indeed, the index of refraction variation due to the Pockels effect in an x-cut lithium niobate substrate in which electrodes are on the substrate surface can be written

$$\Delta n = -\frac{1}{2} n_e^3 r_{33} f_{opt}^2 f_{el} \frac{V}{L} \quad (1)$$

where, $n_e = 2.138$ is the index of refraction of lithium niobate, $r_{33} = 30 \text{ pm/V}$ is the electro-optic coefficient, f_{el} and f_{opt} are the local electrical and optical field factors respectively, V is the external applied voltage and L is the distance between both electrodes.

The number of rows of holes at each side of the Fabry-Perot cavity is going to modify the transmission of the cavity mode as well as the local field enhancement. FDTD numerical simulations have been performed for different number of rows of holes in order to determine the geometry to be fabricated. Results are displayed in Table 1. A good compromise between light transmission and local field factor is found for 5 rows of holes at each side of the defect line (calculated transmission is 92% and local field factor, f_{opt} , is equal to 3).

Table 1. FDTD calculations of the transmission of the guided mode and optical local field factor as a function of the number of rows along the propagation direction

Number of rows	Normalized transmission	Optical local field factor
5	92%	3.02
6	75%	4.03
7	50%	4.82

2.3 Optical and electrical local field factor

In all the works in which local field factor has been calculated for the electro-optic effect, the assumption that the local field enhancement of the optical field was the same as for the electric field has been made. In this paper we have calculated separately both local field factors to validate the hypothesis.

In order to calculate the local electric field factor f_{el} inside the Fabry-Perot photonic crystal geometry, finite element numerical method COMSOL has been used. X-cut lithium niobate has been considered as substrate. Thus, in order to have the highest electro-optic

coefficient, electrodes have to be deposited on the substrate surface and placed parallel to the light propagation. For illustration purposes, an external voltage of 10 V has been assumed to perform the calculations. The photonic crystal consists of 5 lines of holes at each side of the line cavity. Numerical simulation results can be seen in Fig. 3. From the electric field map distribution we can observe that electric field is twice more confined inside the photonic crystal wire than elsewhere. The calculated average electric local field factor within the photonic crystal has a value around 2, which is quite similar to the calculated local optical field factor.

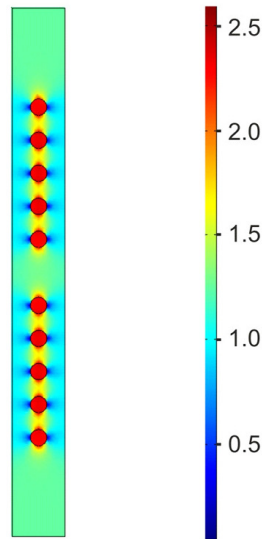


Fig. 3. Finite element numerical simulation of the electrostatic field distribution on the photonic crystal ridge wire waveguide.

3. Device fabrication

The starting material for device fabrication is thin film lithium niobate (TFLN) bonded to a lithium niobate handle wafer as procured from SRICO. The lithium niobate film is formed on the handle wafer using an ion slicing process similar to that used by SOITEC to produce commercial silicon on insulator (SOI) wafers. In the SOITEC process, hydrogen ions are implanted below the surface of a silicon seed wafer at a depth determined by the ion implant energy. After bonding the implanted surface to a handle wafer, the sample is heated in stages until separation of the silicon crystal occurs along the implant plane. This leaves a thin layer of the seed silicon wafer attached to the handle substrate. After annealing and chemical mechanical polishing to remove residual surface damage, the transferred layer is of the same quality as the starting bulk seed wafer. Dubbed “Smart Cut™”, the process has many benefits, including highly uniform film thickness, bulk crystal quality, and tunable film thickness from submicron to over 10 microns. SRICO has utilized ion slicing techniques such as smart-cut to produce TFLN as well as thin films of other materials, such as thin film lithium tantalate (TFLT) [16] for pyroelectric detectors [17] and thin film gallium arsenide (TFGAS) [18] for nonlinear optical applications. Pyroelectric detectors based on TFLT have been proven to exhibit material properties in a very thin film that are equal to that of bulk, resulting in detectivity performance 20 times higher than state of the art commercial devices. Similarly, optical modulators fabricated in TFLN have been shown to retain bulk crystal electro-optic material properties [12, 19-20].

The details of the photonic crystal wire waveguide fabrication process are given in Fig. 4(a) to (f). At first we realize a chromium mask protection for the ridge wave guide fabrication. A positive e-beam (EB) resist (ZEP) is spin-coated on a thin layer of lithium

niobate. The wave guide is then patterned by EB lithography. The resist is spin coated with an exposure dose of $130\mu\text{m}/\text{cm}^2$ obtaining a final thickness of 480 nm. After EB resist development, a 200 nm thick chromium layer is deposited by evaporation before performing a lift off (Fig. 4(a)).

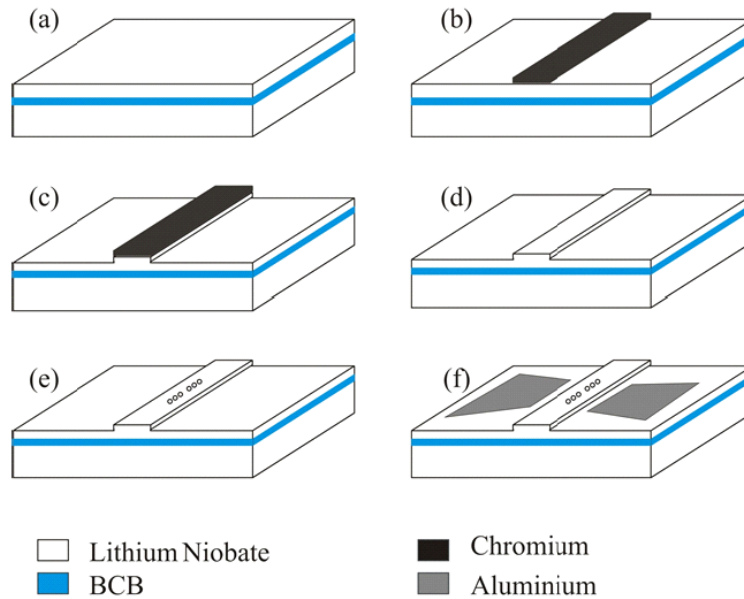


Fig. 4. Flow chart of the ridge waveguide and photonic crystal fabrication stages. Steps (a) to (d) show the ridge waveguide fabrication and steps (e), and (f) the photonic crystal and electrode fabrication.

The mask transfer to the lithium niobate substrate is done by reactive ion etching (RIE). The wire is defined using standard sulfur-hexafluoride-based (SF_6) RIE at low pressure (around 2 μbar) and high power (220 W) (Fig. 4(b) and 4(c)). Finally, the photonic crystal is fabricated with a focused ion beam (FIB) milling (Fig. 4(d)). A Ga + liquid metal ion source (acceleration energy = 30 keV) is used. Ions are focused to the lithium niobate ridge with electrostatic lenses with a probe current of 50-60 pA. In these conditions, the depth of the holes is measured to be $1.5\mu\text{m}$. Here we have to say that the holes exhibit a conical shape: the thicker will be the LN film, the lower will be the overlap coefficient between the waveguide mode and the photonic structure. Increasing the overlap coefficient between the waveguide mode and the photonic structure was one of the major motivations that led us to use thin LN films.

Aluminum electrodes have been deposited at both sides of the photonic crystal (Fig. 4(f)). Due to technological constraints, the distance between electrodes is set to 50 μm , significantly far away from the photonic crystal. The main consequence will be an electro-optic effect that will be reduced since it is inversely proportional to the electrodes distance. A SEM (Scanning Electron Microscope) image of a side and top view of the device can be observed in Fig. 5(a) and (b) respectively.

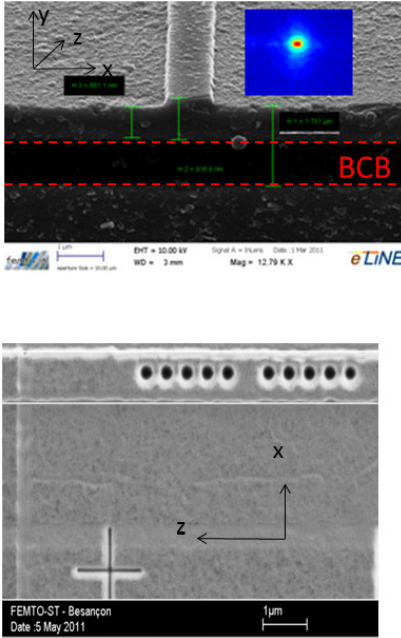


Fig. 5. SEM images of the wire waveguide without (a), and with the photonic crystal cavity (b).

4. Optical characterization

The experimental characterization set-up is the same as in [3] with the only difference of using a lensed fiber to couple light in and out of the lithium niobate thin film. A supercontinuum laser source (wavelength going from 600 to 1700 nm) as well as a tunable IR laser (from 1500 nm to 1610 nm) has been used to couple light into the device. An optical spectrum analyzer and an IR camera have been used to visualize and to detect the transmitted light. Transmission spectrum has been measured for the wire waveguide alone and with the photonic crystal on it. The experimental guided mode visualized with the IR camera at $\lambda = 1550$ nm can be seen in the inset of Fig. 5 (a). The shape and the horizontal extension correspond to the simulated results of Fig. 3(c).

Finally, electro-optical transmission spectrum measurements of the photonic crystal cavity mode for 0V and 30V are shown in Fig. 6(a). It has been normalized with respect to the transmission of the wire waveguide. By the positions of the maxima we believe that the transmission spectrum corresponds to the transmission of the Fabry-Perot resonance cavity. The modulation depth is not as high as it could be expected. We think that this is due to the coupling between the lensed fiber and the photonic wire: as this coupling was not optimized, a part of the injected light is not guided by the wire but is nevertheless measured at the output of the device.

A wavelength shift of 1.2 nm is observed corresponding to an electro-optical enhancement of 18 ($f_{opt}^2 f_{el}$) with respect to bulk material. Here we would like to point out that the application of an external electric field causes a variation of the refractive index, which changes the waveguide mode. As a consequence, the overlap coefficient between the waveguide mode and the photonic structure is also modified, which explains why the spectrum overall shape is slightly modified. This effect also explains why the overall transmission drops significantly in presence of the applied voltage. This shift, that is related to the variation of the index of refraction, corresponds exactly to the calculated wavelength shift by FDTD (simulations of the device fabricated in this work (that is, with a distance between both electrodes of 50 μm) as it is displayed in Fig. 6(b) [4]. Taking into account that the index

of refraction variation in Pockels equation is inversely proportional to the electrodes distance, if we fabricate both electrodes in the vicinity of the photonic crystal (that is with a distance between them of 1 mm) we may expect that only 0.6V will be required for achieving the same wavelength shift of 1.2nm.

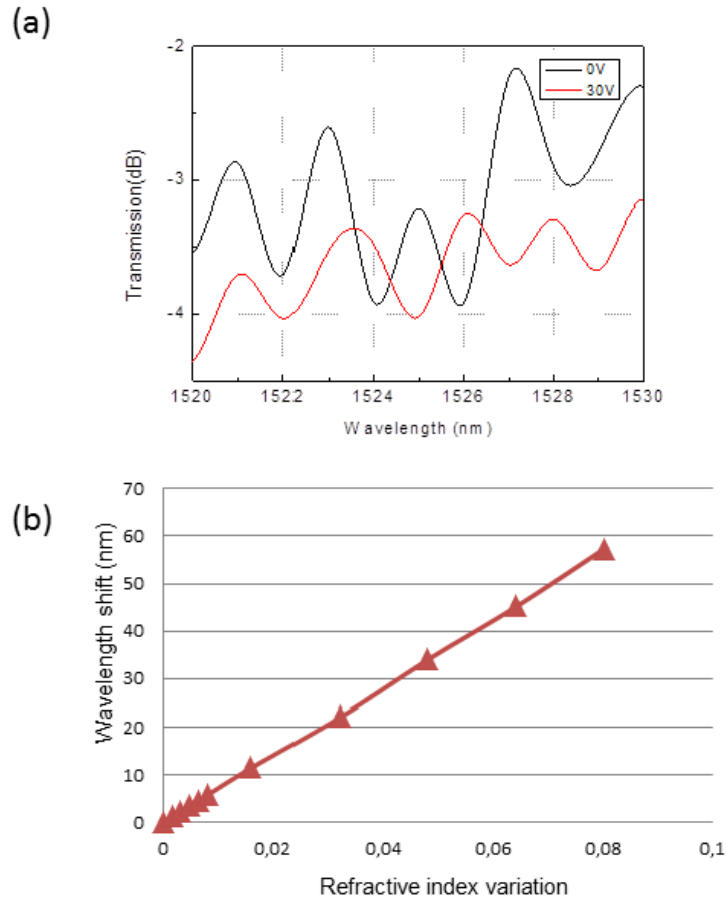


Fig. 6. (a) Experimental transmission spectrum for 0V (black line) and 30V (red line) for the transmission mode of the photonic crystal cavity. (b) FDTD calculation of the wavelength shift of the transmission band as a function of the refractive index variation.

5. Conclusion

In conclusion, we report on a $4 \times 0.8 \mu\text{m}^2$ enhanced electro-optical device based on a slow light lithium niobate photonic crystal wire waveguide. It can potentially shift the transmission band of 57 nm by only applying 30 V of external voltage which is due to a slow light geometry designed on a thin membrane ($1 \mu\text{m}$) of monocrystalline lithium niobate.

Acknowledgments

Huihui LU thanks the Franche Comté region for financial support. This research was sponsored by the Defense Advanced Research Projects Agency, Electric Field Detector (E-FED) Program, issued by DARPA/CMO under Subcontract No: 10103CNRS.